Carbon 130 (2018) 164–169

Contents lists available at ScienceDirect

Carbon

journal homepage: www.elsevier.com/locate/carbon

Flexible graphite films with high conductivity for radio-frequency antennas

Rongguo Song [a, 1], Qianlong Wang [a, b, 1], Boyang Mao [c, 1], Zhe Wang [d], Danli Tang [a], Bin Zhang [a], Jingwei Zhang [a], Chengguo Liu [a], Daping He [a, d, *], Zhi Wu [a, **], Shichun Mu [d]

[a] Hubei Engineering Research Center of RF-Microwave Technology and Application, School of Science, Wuhan University of Technology, Wuhan 430070, China
[b] Shenzhen Institute of Advanced Graphene Application and Technology (SIAGAT), Shenzhen 518106, China
[c] National Graphene Institute, University of Manchester, Booth Street East, Manchester M13 9PL, UK
[d] State Key Laboratory of Advanced Technology for Materials Synthesis and Processing, Wuhan University of Technology, Wuhan 430070, China

ARTICLE INFO

Article history:
Received 25 October 2017
Received in revised form
22 December 2017
Accepted 4 January 2018
Available online 4 January 2018

ABSTRACT

The low conductivity and fragile mechanical toughness of conventional carbon material based films are major barriers for their applications in modern electronics, especially in flexible radio frequency electronics, such as antennas. In order to optimize their performance, the electrical and mechanical properties of the materials need to be improved. In this work, flexible graphite films, fabricated by high temperature thermal treatment of polymer precursor and subsequence compression rolling, are designed and explored to create dipole antennas for radio frequency applications. It is shown that the flexible graphite films with 808.8 $cm^2/V \cdot sec$ carrier concentration have a high conductivity of 1.1×10^6 S/m. We demonstrate that the resulting flexible graphite film dipole antennas can not only produce a relatively high peak gain of 1.45 dB with comparable return loss, bandwidth, and radiation patterns to an identical copper antenna, but also have excellent structure stability and mechanical flexibility. Moreover, the density of the graphite film is 5 times less than the copper film. This indicates that the tailored flexible graphite film could be a new alternative way to produce superb flexible and efficient radio-frequency antennas.

1. Introduction

The research and development of modern electronics is committed to improving the function and reducing the overall size. Flexible radio-frequency (RF) electronics are particularly attractive for the enhanced functionality due to their 'soft' nature in applications such as smart conformal devices and tags [1–3], body-worn wireless electronics [4,5], and the internet of things (IoT) [6]. However, it is important to recognize that the field of flexible RF electronics is still in its infancy, and like most of the emerging electronic technologies, new materials and advanced technologies are the two driving forces for their further developments and practical applications.

Advanced carbon material based films exhibit more favorable properties than most metals in flexibility, mechanical reliability, weight savings and excellent environmental toughness. With such advantages, coupled with excellent electrical conductivity, these flexible carbon-based films have drawn the widespread attention of applications in the next generation of flexible electronic devices. Examples include strain sensors, stretchable transistors, flexible displays [7–9]. And a variety of carbon-based materials including carbon nanotube [10–12], multi-shelled fullerenes [13,14], carbon fibers [15] and graphene [16,17], *etc*. have been used as assembly materials to make films for RF and microwave passive components. Recently, researchers have explored the applications of graphite film to make active electronic devices due to their high electrical conductivity and unique mechanical properties [18–24]. Nevertheless, it is worth to note that the graphite films are limited in their performance owing to high sheet resistance, and is not competitive with commercial metal films yet, particularly in passive electronics such as antenna applications. Because relatively low electrical

* Corresponding author. Hubei Engineering Research Center of RF-Microwave Technology and Application, School of Science, Wuhan University of Technology, Wuhan 430070, China.
** Corresponding author.
E-mail addresses: hedaping@whut.edu.cn (D. He), z.p.wu@whut.edu.cn (Z. Wu).
[1] These authors contributed equally to this work.

https://doi.org/10.1016/j.carbon.2018.01.019
0008-6223/

conductivity will lead to more losses of the device itself and lower radiation efficiency and gain, particularly in passive electronics [25–27]. A latest report established that brilliant thermal and electron conductivity flexible graphene films could be achieved by high temperature treatment of the precursor graphene oxide (GO) films [28]. It can be found that the high temperature (~2000 °C) annealing process improves both thermal and electronic properties of graphene films, and it also leads to flexible graphite film or multilayer graphene like structure due to the repaired layer structure.

Inspired by flexible graphite film fabrication technique reported in 1990s [29], we designed and prepared a flexible graphite film (FGF) with an electrical conductivity as high as ~10^6 S/m by carbonizing and graphitizing a polymer film, in this study polyimide. The post-treats product owing to its high in-plane oriented structure endows the FGF with excellent planar electrical conductivity and low sheet resistant. To our best knowledge, the FGF has few initial works apply to antenna and other passive devices. More importantly, due to its high flexibility and excellent mechanical strength, the FGF can be processed into any desirable shapes. This overcomes the crucial fragile disadvantages that carbon based films normally have.

In this paper, for the first time, we report to the fabrication of FGF thermal annealing and roll compressing of a polyimide membrane with the consideration of applications in flexible antennas. With many advantageous features, the resultant highly flexible FGF show excellent conductivity, low surface resistance, light weight, strong stability, and environmental protection. The FGF dipole antenna performance in terms of gain and return loss compares favorably with various carbon material based antennas reported so far. It is also important to point out that the ultra-thin FGF is attractive because of its high antenna performance (comparable to copper antenna) and its relative simplicity for antenna design and fabrication. This work will be of great significance for wireless communication and the environment.

2. Experimental

2.1. Preparation of FGF

The FGF is prepared in the following three steps: Firstly, the structurally concerned polyimide precursor (PI membrane) is slowly heated to 1300 °C in a continuously vacuumed electric furnace to decompose non-carbon atoms and form amorphous carbon structure (carbonization) for 5–8 h. Secondly, the electric conductivity is further improved by firing the carbonized structure at ultra-high temperature (2850 °C) under Ar atmosphere lead to the graphitic structure with completely generated C-C sp^2 hybridizations. Finally, a rolling process, is firstly introduced here to further get a high oriented FGF with densely packed structure.

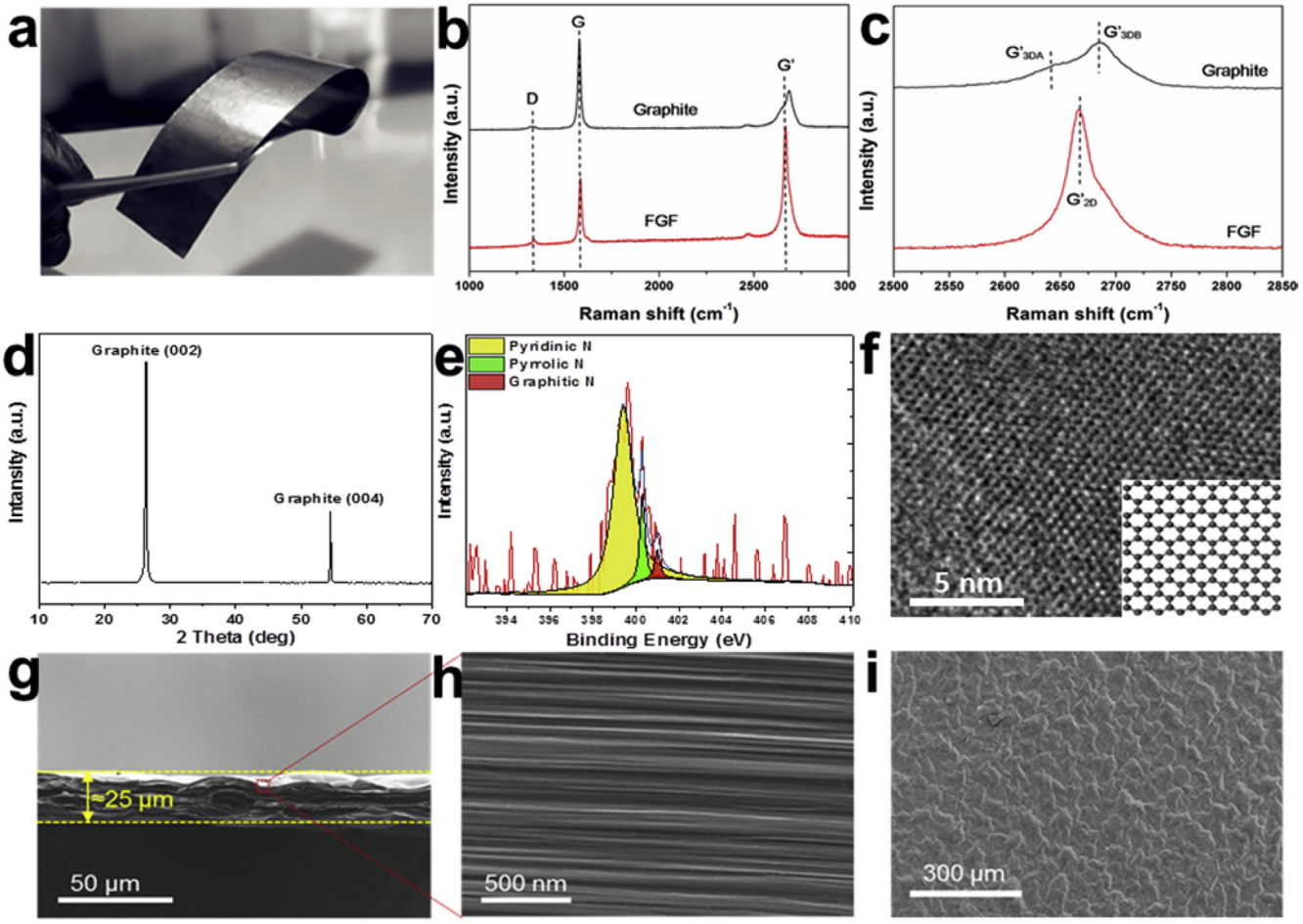

Fig. 1. (a) Digital photograph of FGF; (b, c) Raman and zoomed Raman spectras of FGF and Graphite; (d) XRD patterns of FGF; (e) XPS spectra corresponding to N1s region for the FGF; (f)HRTEM of exfoliated FGF; (g, h) SEM images showing the cross-section of FGF with highly in-plane oriented structure and (i) The surface morphology of FGF. (A colour version of this figure can be viewed online.)

Table 1
Resistivity and conductivity of FGF and copper.

Samples	Thickness [μm]	Resistivity [Ω·m]	Conductivity [S/m]	Density [g/cm^3]
FGF	~25	9×10^{-7}	1.1×10^{6}	1.8
Copper	28	7.5×10^{-8}	1.3×10^{7}	8.8

2.2. Characterization

X-ray diffraction (XRD) patterns were recorded in a Polycristal PANalytical X'Pert Pro apparatus using Ni-filtered Cu Kα radiation. Raman spectra were measured using an excitation wavelength of 457.9 nm provided by a Spectra-Physics Model 2025 argon ion laser. X-ray photoelectron spectroscopy (XPS) was measured on a ESCALAB 250Xi instrument with monochromatic Al Kα Morphological and structural information was analysed with a JEOL JEM6700 scanning electron microscopy (SEM) and high-resolution transmission electron microscopy (HRTEM, JEM-2100F).

3. Results and discussion

Fig. 1a shows a piece of rolled FGF, which demonstrates that FGF have good flexibility and could be fabricated into a variety of shapes and sizes according to the antenna design. The Raman spectras of FGF and commercial graphite film are shown and compared in Fig. 1b and c. In the spectra, FGF exhibits an intense G-band peak at ~1580 cm^{-1}, which is a fingerprint for the high crystalline graphite. The intensity of D-band peak is much weaker than G-band peak, indicating a minims disorder degree of graphitic structure. This is also consistent with the obtained high G′-band (~2700 cm^{-1}) from the second-order Raman scattering [28]. In our fabrication process, the graphitization was carried out at 2850 °C, ending with a coalescence of neighboring sheets into continuous larger sheet (see scheme in supporting materials, Fig. S2), which was confirmed by the experiments carried out by Barreiro et al. [30,31]. Such structural transformation, demonstrates that a graphite film can be fabricated from polyimide film through this graphitization process. Unlike pristine graphite with AB Bernal stacking reflected by a highly asymmetric G′-band that can be fitted into two Lorentzian peaks (G′3DA and G′3DB, Fig. 1c), FGF possesses a completely symmetric G′-band that can only be fitted into a single Lorentzian peak (G′2D, Fig. 1c), revealing the presence of turbostratic stacking between graphite layers due to the random overlaps of polyimide film [32]. The XRD pattern of the FGF is shown in Fig. 1d. It can be seen that the diffraction peaks of FGF are very sharp and intense. The well-marked characteristic graphitic peak is located at around 26.5°, this not only exhibits an interlayer spacing (002) of 0.33 nm, but also indicates a more regular packing of graphene layers with longer correlation length due to the coalescence process after the high temperature annealing [31]. The considerably strong diffraction peak (004) also reflects a high degree of graphitization of FGF. It is worth to note that, the film is nearly fully graphitized, the film still presents a slight N doping (0.54 at%) confirmed by XPS measurements by XPS measurements (Fig. 1e and Fig. S3) due to the initial polyimide precursor, and the detailed data of N percentage change under different annealing temperature as shown in Table S1. In our case, the slightly N doped film could contribute to its high electrical conductivity. To further demonstrate the FGF film structure, this conducting film was applied to a well-studied electrochemistry exfoliation process to get single layer graphene sheets [33]. From the HRTEM and TEM image of exfoliated graphene sheet (Fig. 1f and Fig. S4), the sp^2 graphitic structure can be clearly seen. This confirms that the basic assembly layer structure in FGF film is single graphene sheet and polyimide has transferred entirely into graphitic structure. The morphology of FGF nanostructure is then characterized by SEM. As shown in Fig. 1g and h, the cross-section SEM images of the FGF represents quite thin film of ~25 μm

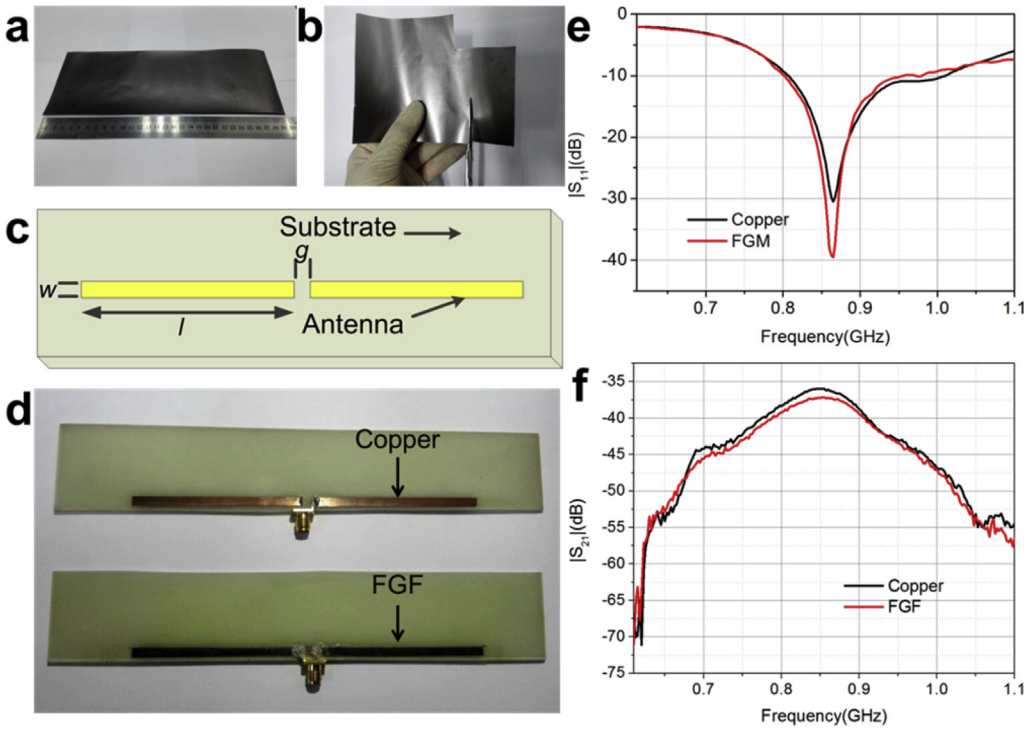

Fig. 2. (a) Photo of FGF; (b) Photo of FGF for cutting; (c) The model of dipole antenna; (d) Photo of the FGF and copper antenna; (e) Measured $|S_{11}|$ of the antennas; (f) Measured $|S_{21}|$ of the antennas. (A colour version of this figure can be viewed online.)

thickness and a typical ordered stacking structure of graphene layers. This reflects a highly in-plane oriented structure and alignment of aromatic segments parallel to the basal plane, which is in good agreement with the appearance of typical (002) and (004) peaks in XRD pattern. Fig. 1i shows that the surface of FGF appears to be rough in microscale.

The electrical conductivity of FGF is verified by the four-probe detection (supporting materials, Fig. S1). As shown in Table 1, the FGF possesses excellent electrical conductivity of 1.1×10^6 S/m and surface resistance of 2.5×10^{-2} Ω/sq, close to copper conductivity (1.3×10^7 S/m). The carrier concentration of the FGF is 808.8 cm^2/V·sec, which measured by Physical Property Measurement System (PPMS-9). This feature indicates that the FGF can be applied to make a good performance antenna. In Table 1, the film density of FGF and copper are presented and compared. It can be seen that the FGF is much lighter (around 5 times) than the copper as the density of FGF is 1.8 g/cm^3 while the copper is 8.8 g/cm^3. The light-weight nature of FGF is a huge advantage in applications such as wearable electronic devices.

Fig. 2a and b shows that the flexible FGF can be simply cut into required shapes for different kinds of antenna designs. The design of dipole antenna on FR-4 PCB substrate (Anhui Lianruan Education Technology Co., Ltd.) is shown in Fig. 2c. The length of the arms l is 68.82 mm, and the arm width w is 3.53 mm. The gap between the two arms g is 3.53 mm. The FR-4 PCB has a dielectric constant of 4.4 and thickness of 1.6 mm. To measure the performance, two arms of the dipole antennas are connected by a SMA connector via conductive adhesive (DOUBLE-BOND CHEMICAL DB2013). Fig. 2d shows the FGF and copper dipole antennas of the same size made on the FR-4 PCB substrate. The reflection coefficients ($|S_{11}|$) of the FGF dipole antenna and copper dipole antenna are measured in microwave anechoic chamber with a Network Analyzer (PNA, Keysight N5225A). As shown in Fig. 2e, the resonant frequencies of both antennas occur at 865 MHz, while the FGF antenna has a smaller reflection coefficient of −39.53 dB than that of copper antenna (−30.51 dB). The −10 dB bandwidth of FGF is from 0.8 GHz to 0.96 GHz, which implies that above 90% power of the antenna is transmitted in this band. Moreover, the fractional bandwidth (*FBW*) of the antenna can be calculated by Ref. [34].

$$FBW = (f_2 - f_1)/f_0 \quad (1)$$

where f_2 is the upper frequency of −10 dB bandwidth, f_1 is the lower frequency of −10 dB bandwidth and f_0 is the resonant frequency of antenna. The results obtained by equation (1) shows that the FGF antenna has a similar *FBW* (20.5%) with the copper antenna (23.4%). In addition to *FBW*, the gain (G) is also an important parameter of the antenna performance. Before measuring the gain,

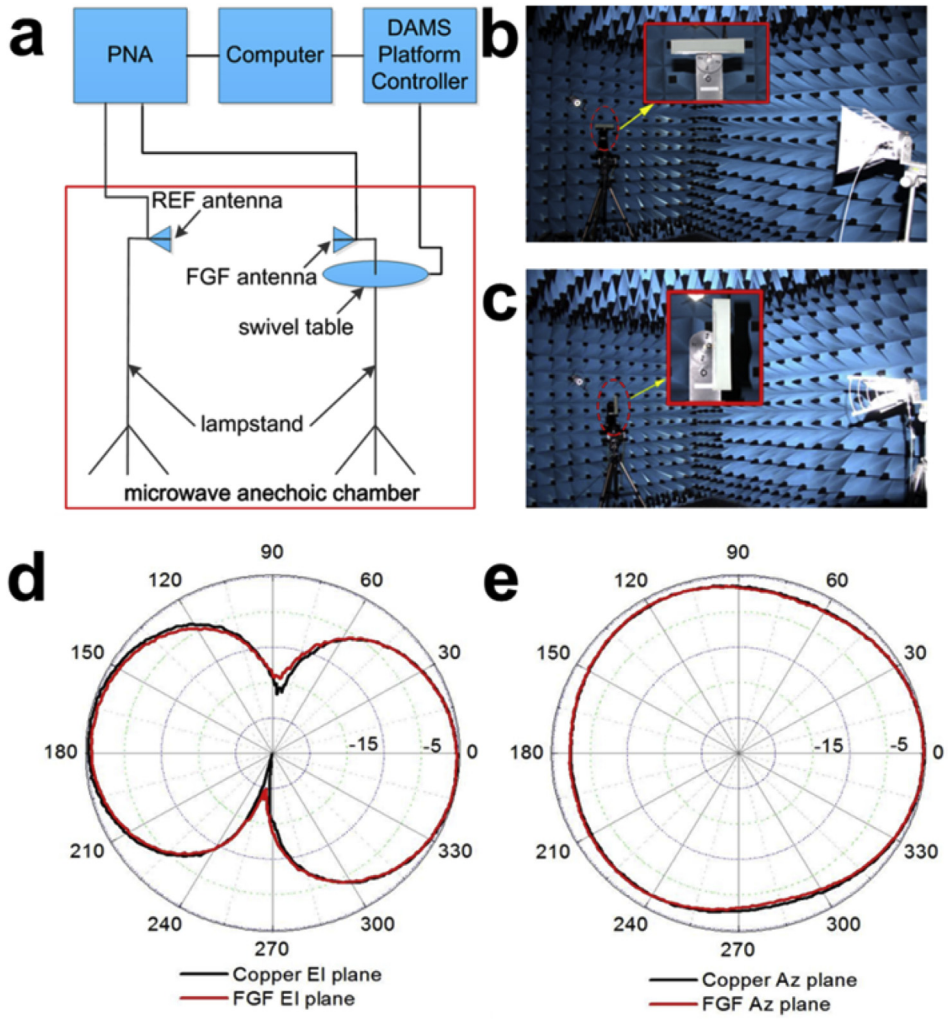

Fig. 3. Radiation pattern measurement in microwave anechoic chamber. (a) Schematic diagram of test system; (b) Photo of Elevation plane measurement; (c) Photo of Azimuth plane measurement; (d) Elevation plane of antennas; (e) Azimuth plane of antennas. (A colour version of this figure can be viewed online.)

the PNA is calibrated with the 85033E calibration of Keysight in order to compensate the loss of the coaxial connection and the adapter. The method used in this paper is to place two identical antennas in the microwave anechoic chamber with a separation distance *r*. Fig. 2f shows the forward transmission coefficient ($|S_{21}|$) of two identical antennas. The gain of the antennas at the resonance point can be calculated using the following equations [34].

$$|S_{21}|(\mathrm{dB}) = P_L(\mathrm{dB}) + 2G(\mathrm{dB}) \tag{2}$$

$$P_L = 20\log(\lambda/4\pi r) \tag{3}$$

where P_L is path loss in dB, λis the wavelength at the resonant frequency, G(dB) is the gain in dB. After applying equations (2) and (3), the gain of the FGF antenna is determined to be 1.45 dB at 865 MHz, which is higher than that of many other carbon material based dipole antennas (Fig. S5), and similar to that of the copper antenna of 1.94 dB.

To further investigate the performance of FGF antenna, the radiation pattern at 865 MHz is measured in the microwave anechoic chamber. The schematic diagram of antenna measurement system is shown in Fig. 3a, The FGF antenna and standard reference antenna are connected with the PNA. The FGF antenna is placed on the turn table as a receiver, and the standard reference antenna (REF antenna) is fastened on the stand as a radiator. The PNA and the antenna measurement system (Diamond Engineering Autonated Measurement Systems) are connected with a GPIB for real-time data reading and analyzing. It should be noted that the turn table is controlled by the DAMS platform Controller, and the resolution for both Azimuth (Az) and Elevation (El) plane is 1°. The measurements are made in the microwave anechoic chamber, as shown in Fig. 3b and c. The Elevation planes of the FGF antenna and copper antenna are shown in Fig. 3d, and the Azimuth planes in Fig. 3e. It can be concluded from the plots that FGF antenna and copper antenna have the same radiation patterns. The FGF based dipole antenna reported here shows a comparable performance to Copper antenna may be readily generalized to other radio-frequency antennas such as microstrip antennas (Supplementary Figs. S6 and S7).

To investigate the flexible property and its effects on electrical conductivity stability of FGF, the film volume resistance after bending is measured, as shown in Fig. 4a. The FGF and wires are fixed within two insulated clamps. Volume resistance is measured by using a digital multimeter (Agilent U1242B). The electrical resistance of FGF does not change after 100 times folding, which demonstrates its significant performance stability. By the way, the resistance of FGF is constant during the bending process, as shown in Fig. S8. The copper foil with same thickness is broken after twelve times bending, as shown in Fig. S9. As also presented in Fig. 4b and Fig. S10, the reflection coefficient of FGF antenna is not affected after 100 times bending. As aforementioned, bending the dipole antenna horizontally shows negligible impact on the material property and antenna performance. Without losing the generality, a more sophisticated antenna, an ultra-wideband coplanar antenna with a potential application onto human's arm (see supporting material, Fig. S11) is designed and bent in both horizontal and vertical directions. The dimensions and fabrication process of ultra-wideband coplanar antenna are shown as Fig. 4c. A LPKF laser engraver machine is used to outline the antenna patch on a PET substrate with dimension of 26 mm*26 mm*0.06 mm. By using the same PNA, the reflection coefficients ($|S_{11}|$) of this flexible FGF ultra-wideband coplanar antenna in different situations are measured in anechoic chamber. As it can be seen in Fig. 4d, bending in different directions are conducted and there is no significant influence on

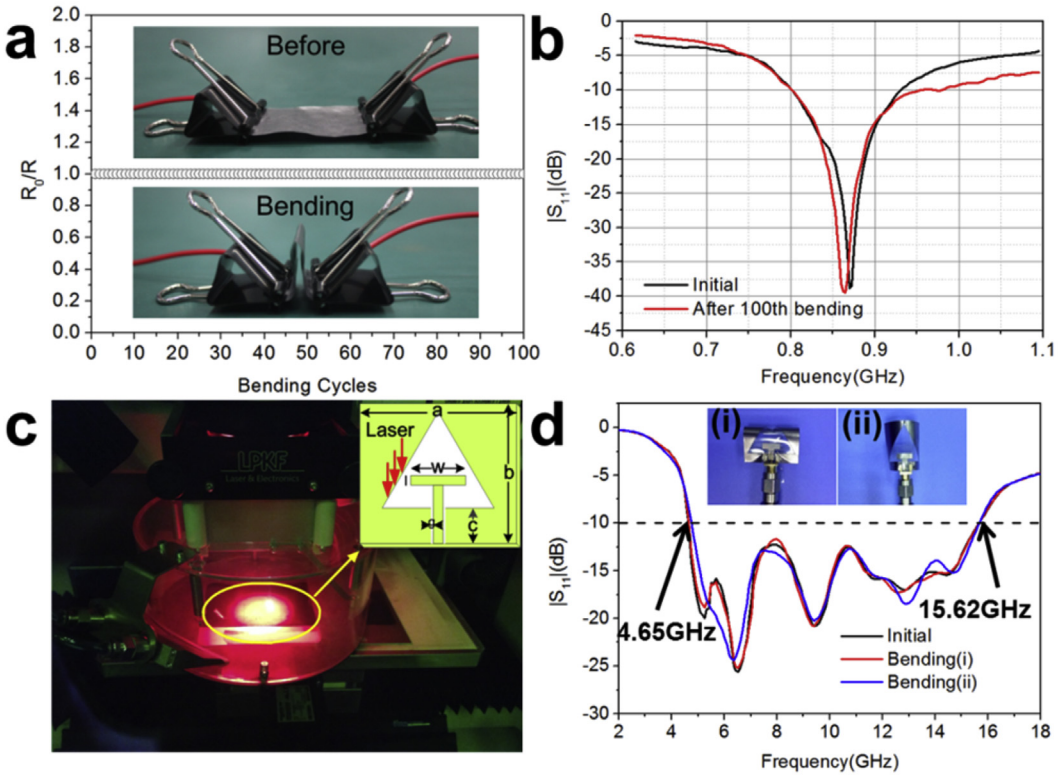

Fig. 4. (a) Resistance change of FGF with bending test; (b) $|S_{11}|$of the FGF antenna (before and after bending); (c) The dimensions and fabrication process of FGF ultra-wideband coplanar antenna. a = b = 26 mm, c = 4.71 mm, w = 8.5 mm, l = 3 mm, g = 0.35 mm; (d) Performance comparison of initial/bending FGF ultra-wideband coplanar antenna. (A colour version of this figure can be viewed online.)

antenna performance as both curves of two bending cases show good agreement with the original one. The values of −10 dB bandwidth for three cases range from 4.65 GHz to 15.62 GHz, which also prove that the FGF material has excellent conductivity as well as high flexibility.

4. Conclusion

In conclusion, this work for the first time demonstrates a flexible graphite film (FGF) fabricated by high temperature annealing and compression rolling of polyimide can serve as a dipolar antenna with an excellent performance, better than those reported using carbon nanotubes, fullerene and other carbon nanomaterials based film. The FGF antenna possesses a gain as high as1.45 dB which is comparable to its copper counterpart (1.94 dB). At the same time, the FGF exhibits a significant stability in electrical conductivity and reflection coefficient during the bending test. This suggests its promising application as a new alternative material in flexible radio-frequency antennas. In addition, the FGF is easy to process into any kind of shapes to meet sophisticate antenna design requirements. The density of FGF is also lighter than copper film. During the synthesis process, it is noted that the polymer precursor can be adjusted accordingly and the film making technique can be expended and applied to other 2D materials. Thus, this research has demonstrated that the FGF has great potential in antenna design and radio-frequency applications.

Acknowledgements

The authors acknowledge financial support from the National Natural Science Foundation of China (51701146, 516722040), the Natural Science Foundation of Hubei Province of China (2015CFB719) and the Fundamental Research Funds for the Central Universities (WUT:2017IB015). We also acknowledge the Center for Materials Research and Analysis of Wuhan University of Technology for TEM (Dr. Xiaoqing Liu) and picture suggestions.

Appendix A. Supplementary data

Supplementary data related to this article can be found at https://doi.org/10.1016/j.carbon.2018.01.019.

References

[1] D.-H. Kim, J. Viventi, J.J. Amsden, J. Xiao, L. Vigeland, Y.-S. Kim, J.A. Blanco, B. Panilaitis, E.S. Frechette, D. Contreras, et al., Dissolvable films of silk fibroin for ultrathin conformal bio-integrated electronics, Nat. Mater. 9 (2010) 511–517.
[2] D. Akinwande, N. Petrone, J. Hone, Two-dimensional flexible nanoelectronics, Nat. Commun. 5 (2014) 5678.
[3] D. Akinwande, L. Tao, Q. Yu, X. Lou, P. Peng, D. Kuzum, Large-area graphene electrodes: using CVD to facilitate applications in commercial touchscreens, flexible nanoelectronics, and neural interfaces, IEEE Nanotechnol. Mag. 9 (2015) 6–14.
[4] L. Gatzoulis, I. Iakovidis, Wearable and portable eHealth systems, IEEE Eng. Med. Biol. Mag. 26 (2007) 51–56.
[5] S.W. Hwang, D.H. Kim, H. Tao, T. Il Kim, S. Kim, K.J. Yu, B. Panilaitis, J.W. Jeong, J.K. Song, F.G. Omenetto, et al., Materials and fabrication processes for transient and bioresorbable high-performance electronics, Adv. Funct. Mater. 23 (2013) 4087–4093.
[6] A. Nathan, A. Ahnood, M.T. Cole, S. Lee, Y. Suzuki, P. Hiralal, F. Bonaccorso, T. Hasan, L. Garcia-Gancedo, A. Dyadyusha, et al., Flexible electronics: the next ubiquitous platform, Proc. IEEE 100 (2012) 1486–1517.
[7] T. Yamada, Y. Hayamizu, Y. Yamamoto, Y. Yomogida, A. Izadi-Najafabadi, D.N. Futaba, K. Hata, A stretchable carbon nanotube strain sensor for human-motion detection, Nat. Nanotechnol. 6 (2011) 296–301.
[8] B.J. Kim, H. Jang, S.K. Lee, B.H. Hong, J.H. Ahn, J.H. Cho, High-performance flexible graphene field effect transistors with ion gel gate dielectrics, Nano Lett. 10 (2010) 3464–3466.
[9] S.H. Chae, Y.H. Lee, Carbon nanotubes and graphene towards soft electronics, Nano Converg. 1 (2014) 15.
[10] C. Rutherglen, D. Jain, P. Burke, Nanotube electronics for radiofrequency applications, Nat. Nanotechnol. 4 (2009) 811–819.
[11] T.A. Elwi, H.M. Al-Rizzo, D.G. Rucker, E. Dervishi, Z. Li, A.S. Biris, Multi-walled carbon nanotube-based RF antennas, Nanotechnology 21 (2010) 45301.
[12] I. Puchades, J.E. Rossi, C.D. Cress, E. Naglich, B.J. Landi, Carbon nanotube thin-film antennas, ACS Appl. Mater. Interfac. 8 (2016) 20986–20992.
[13] N.A. Vacirca, J.K. McDonough, K. Jost, Y. Gogotsi, T.P. Kurzweg, Onion-like carbon and carbon nanotube film antennas, Appl. Phys. Lett. 103 (2013) 1–5.
[14] O. Shenderova, V. Grishko, G. Cunningham, S. Moseenkov, G. McGuire, V. Kuznetsov, Onion-like carbon for terahertz electromagnetic shielding, Diam. Relat. Mater. 17 (2008) 462–466.
[15] A. Mehdlpour, C.W. Trueman, A.R. Sebak, S.V. Hoa, Carbon-fiber composite t-match folded bow-tie antenna for RFID applications, in: IEEE Antennas and Propagation Society, AP-S International Symposium (Digest), 2, 2009, pp. 2–5.
[16] S.Z. Sajal, B.D. Braaten, V.R. Marinov, A microstrip patch antenna manufactured with flexible graphene-based conducting material, in: IEEE Antennas and Propagation Society, AP-S International Symposium (Digest) 2015, 2015–Octob, pp. 2415–2416.
[17] S.N.H. Sa'don, M.R. Kamarudin, F. Ahmad, M. Jusoh, H.A. Majid, Graphene array antenna for 5G applications, Appl. Phys. Mater. Sci. Process 123 (2017) 1–4.
[18] T. Takeichi, Y. Eguchi, Y. Kaburagi, Y. Hishiyama, M. Inagaki, Carbonization and graphitization of BPDA/PDA polyimide films: effect of structure of polyimide precursor, Carbon 37 (1999) 569–575.
[19] A.R. Ubbelohde, Carbons as a route to synthetic metals, Carbon 14 (1976) 1–5.
[20] Y. Hishiyama, M. Nakamura, Y. Nagata, M. Inagaki, Graphitization behavior of carbon film prepared from high modulus polyimide film: synthesis of high-quality graphite film, Carbon 32 (1994) 645–650.
[21] T. Ohnishi, I. Murase, T. Noguchi, M. Hirooka, Highly conductive graphite film prepared from pyrolysis of poly(p-phenylene vinylene), Synth. Met. 14 (1986) 207–213.
[22] T. Ohnishi, I. Murase, T. Noguchi, M. Hirooka, Preparation of graphite film by pyrolysis of polymers, Synth. Met. 18 (1987) 497–502.
[23] C.B. Labelle, K.K. Gleason, Surface morphology of PECVD fluorocarbon thin films from hexafluoropropylene oxide, 1,1,2,2-tetrafluoroethane, and difluoromethane, J. Appl. Polym. Sci. 74 (1999) 2439–2447.
[24] M. Murakami, Y. Yumoto, S. Mizogami, H. Yasujima, S. Naitoh, S. Yoshimura, Thermal Decomposition and Carbonization Mechanism of Poly-para-phenyleneoxadiazole, J. Polym. Sci. Polym. Chem. 28 (1990) 1483–1493.
[25] T. Leng, X. Huang, K. Chang, J. Chen, M.A. Abdalla, Z. Hu, Graphene nanoflakes printed flexible meandered-line dipole antenna on paper substrate for low-cost RFID and sensing applications, IEEE Antenn. Wireless Propag. Lett. 15 (2016) 1565–1568.
[26] M. Akbari, M.W.A. Khan, M. Hasani, T. Bjorninen, L. Sydanheimo, L. Ukkonen, Fabrication and characterization of graphene antenna for low-cost and environmentally friendly RFID tags, IEEE Antenn. Wireless Propag. Lett. 15 (2016) 1569–1572.
[27] X. Huang, T. Leng, X. Zhang, J.C. Chen, K.H. Chang, A.K. Geim, K.S. Novoselov, Z. Hu, Binder-free highly conductive graphene laminate for low cost printed radio frequency applications, Appl. Phys. Lett. 106 (2015).
[28] B. Shen, W. Zhai, W. Zheng, Ultrathin flexible graphene film: an excellent thermal conducting material with efficient EMI shielding, Adv. Funct. Mater. 24 (2014) 4542–4548.
[29] M. Murakami, N. Nishiki, K. Nakamura, J. Ehara, H. Okada, T. Kouzaki, K. Watanabe, T. Hoshi, S. Yoshimura, High-quality and highly oriented graphite block from polycondensation polymer films, Carbon 30 (1992) 255–262.
[30] A. Barreiro, F. Börrnert, M.H. Rümmeli, B. Büchner, L.M.K. Vandersypen, Graphene at high bias: cracking, layer by layer sublimation, and fusing, Nano Lett. 12 (2012) 1873–1878.
[31] A. Barreiro, F. Börrnert, S.M. Avdoshenko, B. Rellinghaus, G. Cuniberti, M.H. Rümmeli, L.M.K. Vandersypen, Understanding the catalyst-free transformation of amorphous carbon into graphene by current-induced annealing, Sci. Rep. 3 (2013) 1115.
[32] S. Reich, C. Thomsen, Raman spectroscopy of graphite, Phil. Trans. Math. Phys. Eng. Sci. 362 (2004) 2271–2288.
[33] H.C. Semmelhack, R. Höhne, P. Esquinazi, G. Wagner, A. Rahm, K.H. Hallmeier, D. Spemann, K. Schindler, Growth of highly oriented graphite films at room temperature by pulsed laser deposition using carbon-sulfur targets, Carbon 44 (2006) 3064–3072.
[34] Gary A. Thiele, Antenna Theory and Design, Wiley, 1981.